

#### Contents lists available at ScienceDirect

# **Fuel**

journal homepage: www.elsevier.com/locate/fuel



## Full Length Article

# Investigation of Ni/Fe/Mg zeolite-supported catalysts in steam reforming of tar using simulated-toluene as model compound



Talal Ahmed<sup>a</sup>, Shuangning Xiu<sup>b,\*</sup>, Lijun Wang<sup>b,c</sup>, Abolghasem Shahbazi<sup>b,c,\*</sup>

- <sup>a</sup> Department of Nanoengineering (Joint School of Nanoscience and Nanoengineering), North Carolina A & T State University, 2907 E. Gate Blvd, Greensboro, NC 27401, United States
- <sup>b</sup> Biological Engineering Program, Department of Natural Resources and Environmental Design, North Carolina A & T State University, 1601 East Market Street, Greensboro, NC 27411, United States
- <sup>c</sup> Department of Chemical, Biological, and Bioengineering, North Carolina A & T State University, 1601 East Market Street, Greensboro, NC 27411, United States

#### ARTICLE INFO

#### Keywords: Biomass tar Steam reforming Toluene Ni-Fe-Mg/zeolite Catalyst

## ABSTRACT

Catalytic performance of Ni/zeolite, Ni-Fe/zeolite, and Ni-Fe-Mg/zeolite catalysts were investigated in steam reforming of toluene as a biomass tar model compound to explore promotional effect of MgO and Fe on Ni/zeolite support. The Ni-Fe-Mg/zeolite catalysts with optimum metallic composition showed higher catalytic performance over corresponding monometallic Ni and Fe catalysts and Ni-Fe/zeolite (bimetallic) catalysts. Addition of Mg to Ni-Fe/zeolite catalyst enhanced the tar reforming reactions and increased the carbon deposition tolerance. The results suggest that Ni-Fe/zeolite and Ni-Fe-Mg/zeolite catalysts have great potential for application in the steam reforming of biomass tar.

#### 1. Introduction

In recent years, the utilization of biomass as a renewable and sustainable energy source, particularly the application of municipal solid waste in gasification, has attracted tremendous technical interest [1]. The hydrogen-rich syngas can be used as a fuel for many downstream applications. However, one of the most critical issues in biomass gasification is the formation of tars [2]. Biomass tars cause serious hazards to equipment in downstream applications due to their low condensation temperatures, resulting in activity reduction and an increase in the frequency of maintenance requirements [3]. Therefore, tars should be extensively removed from the effluent stream of biomass gasification

Many processes have been developed to eliminate tar from the syngas stream [5]. The techniques employed are mainly physical and chemical technologies [6,7]. Among these techniques, catalytic steam reforming of biomass tar has attracted many interests as a viable means for reducing biomass tar in the effluent gas of biomass gasification [8]. This technique produces high-value syngas.

The chemical reactions carried out during the tar formation process involve a complex mixture of hydrocarbon decomposition equilibrium reactions. These decomposition reactions involve steam reforming, steam dealkylation, hydrocracking, hydrodealkylation, dry reforming, carbon formation, and many cracking reactions [9].

The  $Ni/SiO_2$  catalysts have been investigated in methanol, ethanol, and for tar reforming resulting in improved syngas yield [10.11].

Catalytic steam reforming has been stated as being a potential technique in tar removal from gaseous products by transformation of tar into hydrogen and carbon monoxide in the presence of steam [2]. The catalytic tar reforming of tar using iron-, cobalt-, and nickel-based catalysts, dolomites, olivine, and catalyst-loaded zeolites has been extensively studied in the catalytic reforming of tar at temperatures in the range of 600-900 °C [2]. Zeolite provided good catalytic activity in the catalytic cracking of tar. A small amount of coke is formed over zeolitesupported catalysts [2]. It has been reported that the Y type of zeolite was capable of removing 100% of tar in catalytic cracking at hightemperature syngas when using 1-methylnaphthalene as a model of the tar compound [2]. The transition metal-impregnated or exchanged zeolite catalysts were applied for partial and deep oxidation of hydrocarbons [2]. The results showed that the transition metal cations improved zeolite activity for hydrocarbon conversion. The hydrocarbon conversion phenomenon is explained by developing strong zeolite acidity and proper oxygen chemisorption [2].

The global search for new feedstocks to supply hydrogen is on the rise. One of the main feedstocks targeted for hydrogen production through reforming is municipal solid waste (MSW) [12]. It is also, one of the promising low-cost raw materials for hydrogen production, by eliminating MSW-derived tar, is the refused derived fuel (RDF) [13].

E-mail addresses: xshuangn@ncat.edu (S. Xiu), ash@ncat.edu (A. Shahbazi).

<sup>\*</sup> Corresponding authors at: Biological Engineering Program, Department of Natural Resources and Environmental Design, North Carolina A&T State University, 1601 East Market Street, Greensboro, NC 27411, United States.

T. Ahmed et al. Fuel 211 (2018) 566-571

The thermal processing of RDF produces a high quality syngas with robust  $H_2$  and CO molar ratio in the effluent gas stream [14]. This valuable syngas can be further used in a variety of applications such as combustion in a micro-turbine for power generation and downstream applications such as Fischer-Tropsch synthesis [15].

The overall goal of this research was to understand the role and mechanism of Ni-Fe-Mg/zeolite catalyst on tar cracking. To the best of our knowledge, Ni-Fe-Mg/zeolite catalyst have not been investigated before.

#### 2. Materials and methods

#### 2.1. Materials and catalyst preparation

Iron (Fe) and nickel (Ni) over zeolite catalysts were prepared by the incipient impregnation method of catalysis [10,14,15]. Aqueous solutions of nickel nitrate tetrahydrate and iron nitrate hexahydrate were used as metal precursors [16]. Different molar ratios of these precursors to zeolite were used, leading to different metal weight concentrations (3–9 wt%). The excess water was initially evaporated at 105 °C. The samples were dried overnight at 105 °C and calcined under air at 500 °C for 4 h before storage for later use. Magnesium (Mg) catalyst over zeolite was prepared by the sequential incipient impregnation method. Aqueous solution of magnesium nitrate tetrahydrate was used as metal precursor. The calcination process was similar to calcined nickel and iron.

The mechanism of Ni-Fe-Mg/Zeolite catalyst on tar cracking is:

Steam reforming: 
$$C_n H_m + nH_2 O \rightarrow nCO + \frac{n+m}{2} H_2$$

# 2.2. Catalyst characterization

## 2.2.1. Programmed reduction (TPR) analysis

The temperature-programmed reduction (TPR) analysis was performed on Autochem 2920 from Micromeritics. Prior to TPR measurement, 0.07 g of catalyst was outgassed in helium for 1 h at 300 °C to remove any impurities, followed by cooling of the sample to room temperature;  $10\%~H_2/Ar$  gas was then introduced to the catalyst as a reductive gas while the furnace temperature was increased at a heating rate of 10 °C/min to 1000 °C. The flow rate of  $H_2/Ar$  was 30 ml/min. The final furnace temperature was held for 30 min. The consumption of  $H_2$  was monitored continuously with TCD gas chromatograph equipped with a dry ice trap in order to remove  $H_2O$  from the effluent gas. The amount of  $H_2$  was measured using the peak area in TPR profiles. Due to the different reduction degrees of Ni/zeolite catalysts, the dispersion degree of Ni (D%) and the average particle size of Ni in reduced form  $(d_{Ni})$  were mainly calculated using the following equations [6]:

$$D\% = \frac{1.17X}{W \times f}$$

And

$$D_{Ni} = \frac{97.1}{D\%}$$

Where X is the  $\rm H_2$  uptake by the catalyst in  $\mu mol/g$ -catalyst, W is the weight percentage of active Ni, and f is the fraction of NiO reduced into Ni (reduction degree).

#### 2.2.2. Temperature-programmed desorption (TPD) analysis

The qualitative and quantitative basicity strength of nickel and iron on zeolite were performed by the most common method in the literature, namely, TPD of CO<sub>2</sub>. CO<sub>2</sub>-TPD profiles were analyzed using a Micromeritics autochem 2920. One hundred mg of Ni-zeolite and Ni-Fe/zeolite were tested by the adsorption of CO<sub>2</sub> at 50 °C for 30 min. The samples of monometallic and bimetallic catalysts were purged in

helium for 30 min. Desorption of  $CO_2$  was carried out during the heating stage of the samples. The heating range was 30 °C–1000 °C. The heating ramp rate was set to 10 °C/min.

#### 2.2.3. X-ray diffraction (XRD) analysis

The crystallographic analysis of mono, bi, and promoted catalysts were carried out using a D8 DISCOVER X-ray diffractometer (Bruker Optics, Inc., Billercia, MA). This instrument is used to study the crystallinity behavior of mono, bi, and promoted catalysts. The diffraction spectra were recorded in a 20 angle range of  $10^{\circ}$ – $70^{\circ}$  with a PSD detector at a scanning rate of  $0.014^{\circ}$ /s. Cu K $\alpha$  radiation ( $\lambda = 1.54$  Å) produced at 40 mA and 40 kV was used as the X-ray source.

#### 2.3. Catalytic activity test

The catalytic reaction was carried out in a fixed bed reactor with an inner diameter of 4 mm and a length of 400 mm. Sample amounts of 0.03 g and 0.07 g were investigated in each test and held by quartz wool placed in the middle of the reactor. In the catalytic steam reforming test that was performed, toluene composition in the affluent stream was 320 µmol. This toluene concentration was attained by diluting the toluene feed stock using nitrogen and H2O in the steam reforming. Prior to the chemical catalytic reaction, the catalyst was reduced in 30 ml/min of hydrogen at 873 K for 6 h. After reduction, the system was purged with 120 ml/min nitrogen while the temperature was kept at the desired temperature of 873 K. Water and toluene were vaporized at a close temperature range. The temperature difference is only 100 °C; therefore, both were preheated and mixed in a preheater at 400 °C. This mixed solution was used to ensure the proper dilution of toluene to create a homogeneous phase of nitrogen and toluene before approaching the reactor chamber. This homogeneous phase is controlled to maintain the vapor state. The reaction products were then passed through a cold trap to condense unreacted toluene and moisture in the effluent stream. The non-condensable gas products were collected using gas sampling bags and analyzed using a GC-TCD type of gas chromatography (7890A) unit from Agilent technologies. The qualitative and quantitative analyses were carried out using the chromatogram of the produced gases. The chromatogram reflects the peak areas for all produced gases which were then converted to a volume percentage through a calibration curve. The gas chromatography is equipped with a thermal conductivity detector. The thermal conductivity detector is mainly used to detect all inorganic gases. The total flow rate of the product gases was measured using a needle bubble flow meter. The conversion of toluene was evaluated in terms of the carbon balance, which was calculated using the following formula [15]:

$$X \text{ toluene}(\%) = \frac{\text{nCO} + \text{nCO}_2}{7 \times \text{nr in}} \times 100$$

where n is molar flow rate of each gas.

# 3. Results and discussion

## 3.1. Characteristics of catalysts

#### 3.1.1. TPR analysis results

The TPR showed that NiO has a reduction peak at 470 °C. This peak has a dramatic decrease after the NiO was supported on zeolite and a new peak was detected at temperatures above 550 °C (Fig. 1). The latter peak was ascribed to the physical interaction between zeolite and NiO, resulting in the increase of reduction temperature. Therefore, Ni and NiO coexist on the surface of zeolite under the annealing temperature of 550 °C. From the TPR study as shown in Fig. 1, all the mon, bi and promoted bimetallic catalysts are reduced at the temperature range between 300 and 700 °C. Therefore, in this work, all catalysts were reduced under  $\rm H_2$  flow at 700 °C for 6 h before use. It is noted that, the doping of nickel with iron seems to decrease the monometallic catalysts



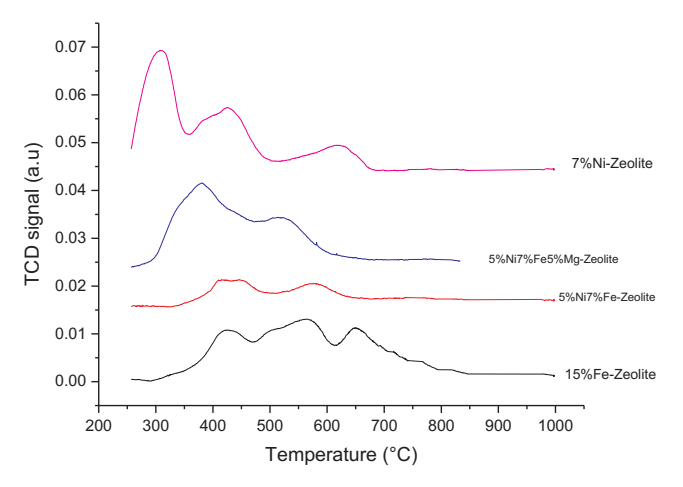


Fig. 1. H<sub>2</sub>-TPR of monometallic versus bimetallic and promoted bimetallic catalysts.

(nickel and iron on zeolite) from 700  $^{\circ}\text{C}$  to 600  $^{\circ}\text{C}$ . Furthermore, addition of magnesium to the bimetallic catalysts further reduced the reduction temperature to 550  $^{\circ}\text{C}$ .

Table 1 shows that almost all the Ni and Fe species are reduced to the metallic state. The reducibility of Fe species on Fe-zeolite is higher than that of Ni species on Ni-zeolite. The simultaneous reduction of Fe and Ni is suggested on Ni-Fe-zeolite catalysts because the presence of Fe promotes the reduction of Ni species. The amount of  $\rm H_2$  adsorption on the freshly synthesized catalysts after the reduction at 973 K and the dispersion are listed in Table 1. Here, it is assumed that most of the Ni and Fe species are reduced and the ratio of hydrogen atom to surface metal is equal to 1. The dispersion that estimated from  $\rm H_2$  adsorption agree with the XRD results. This agreement suggests much likely the existence of homogeneous composition of Ni-Fe solid solution in the catalytic system.

#### 3.1.2. TPD analysis results

The basic strength of Ni-zeolite, Ni-Fe-zeolite and Ni-Fe-Mg-zeolite catalysts was also measured using CO<sub>2</sub>-TPD and the results are presented in Fig. 2. All the profiles in Fig. 2 show similar CO<sub>2</sub> desorption behavior. The CO<sub>2</sub> desorption profile ranged between 100 °C and 600 °C. These peaks can be ascribed to low-strength basic sites, such as bicarbonates that result from chemical interactions between CO<sub>2</sub> and weak basic surface hydroxyl groups [17,18,19,20,21,22]. In Fig. 2 Nizeolite profile has CO<sub>2</sub> desorption peak centered at around 200 °C, whereas the CO<sub>2</sub> desorption peak in Ni-Fe/zeolite and Ni-Fe-Mg/zeolite profiles is slightly shifted toward higher temperatures of 220 °C and 240 °C, respectively. This can be due to the variation of intensity of the basic sites of Ni/zeolite catalyst compared to Ni-Fe/zeolite and Ni-Fe-Mg/zeolite catalysts. Also the geometry of theses active sites plays a crucial role in determining the temperature of CO<sub>2</sub> molecules desorption.

In addition to the desorption peaks at 240 °C, Ni-Fe-Mg/zeolite

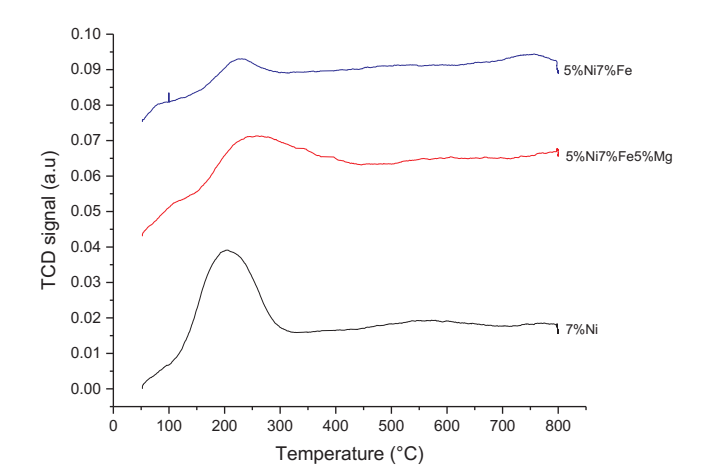


Fig. 2. CO2-TPD of monometallic and bimetallic catalysts.

profile shows an extended desorption peak that is inclined towards high temperature (520 °C). This result suggests Mg plays a role in enhancing the basic strength of Ni-Fe/zeolite system. Furthermore, the  $CO_2$  desorption peak of Ni-Fe/zeolite has a similar behavior as that of Ni/zeolite system due to the presence of higher-than-optimal Fe content. This result suggests that the high catalytic performance of Ni-Fe-Mg/zeolite is likely attributed to its higher basic strength as compared to the rest of catalysts. The basicity of a catalyst increases the catalyst capability to neutralize the acidity of zeolite, thereby suppressing cracking and polymerization known reactions. This suppression in turn leads to enhanced steam-coke reaction.

## 3.1.3. XRD analysis results

The XRD of the reduced catalysts with different Nickel loadings is screened to study the reduced catalyst crystallographic nature. The peaks shown in Fig. 3 at  $2\theta=8.1^\circ$ ,  $13.5^\circ$ ,  $19.6^\circ$ ,  $24^\circ$ , and  $20.7^\circ$  are observed and attributed to zeolite crystals. When Ni/zeolite is reduced at 500 °C, a new crystalline phase is found at  $2\theta=37.1^\circ$ ,  $43^\circ$ , and  $62.4^\circ$  (Fig. 3), which is ascribed to nickel oxide, especially on 10% Ni/zeolite

#### 3.1.4. Thermogravimetric analysis (TGA) of spent catalyst

The deposition of coke over the spent catalysts was studied using thermogravimetric analysis (TGA). Three different stages can be identified with the thermogravimetric and DSC curves (Figs. 4 and 5) when spent catalysts were analyzed. The first stage represents a mass decrease due to water evaporation, which occurs at a temperature below 100 °C. The second stage in this profile corresponds to the Nickel phase oxidation around 350 °C, and finally carbon combustion which occurs at a temperature above 400 °C. Moreover, two types of carbon deposits are suggested to be formed over the catalysts surfaces, namely, amorphous carbon and filamentous carbon. The amorphous carbon oxidation state is shown to initiate around 500 °C, whereas the filamentous carbon

Table 1 Properties of the catalysts after  $H_2$  reduction at 973 K.

Catalyst	Ni/Fe	Content/mmolg <sup>-1</sup> -catalyst		H <sub>2</sub> consumption in TPR <sup>a</sup> /mmolg <sup>-1</sup> -catalyst <sup>b</sup>	Ni-based reduction degree/%	Reduced Fe amount/ mmolg <sup>-1</sup> -catalyst	$ m H_2$ adsorption/ $ m 10^{-6}~mol~g^{-1}$ catalyst	Dispersion/% H/(Ni + Fe)
		Ni	Fe	•				
Ni/zeolite	0	3	0.0	2.4	172	0	29	2.4
Ni-Fe/zeolite	0.6	3	5.0	3.2	141	1.2	22	1.8
	0.71	5	7.0	3.8	115	0.48	15	0.8
	0.77	7	9.0	4.6	92	0.21	10	0.5
Fe/Zeolite	_	_	5.0	0.3	_	1.4	_	_

<sup>&</sup>lt;sup>a</sup> The stoichiometry assumed is: Ni<sup>2+</sup> + H<sub>2</sub>  $\rightarrow$  Ni<sup>0</sup> + 2H<sup>+</sup> and Fe<sub>3</sub>O<sub>4</sub> + 4H<sub>2</sub>  $\rightarrow$  3Fe + 4H<sub>2</sub>O.

<sup>&</sup>lt;sup>b</sup> The consumption below 773 K in TPR profiles shown in Fig. 4.

T. Ahmed et al. Fuel 211 (2018) 566–571

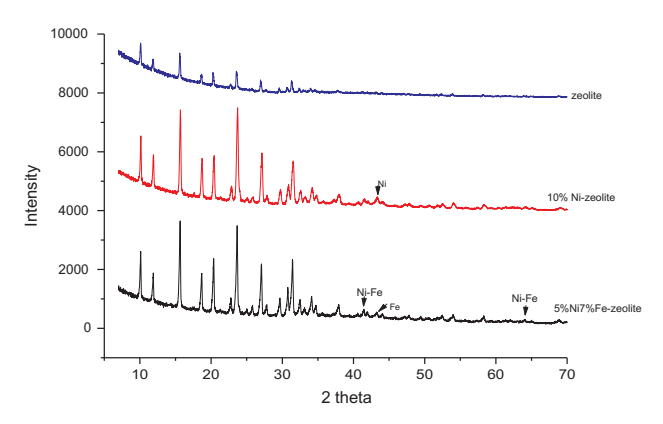


Fig. 3. XRD of mono and bimetallic catalysts compared to zeolite.

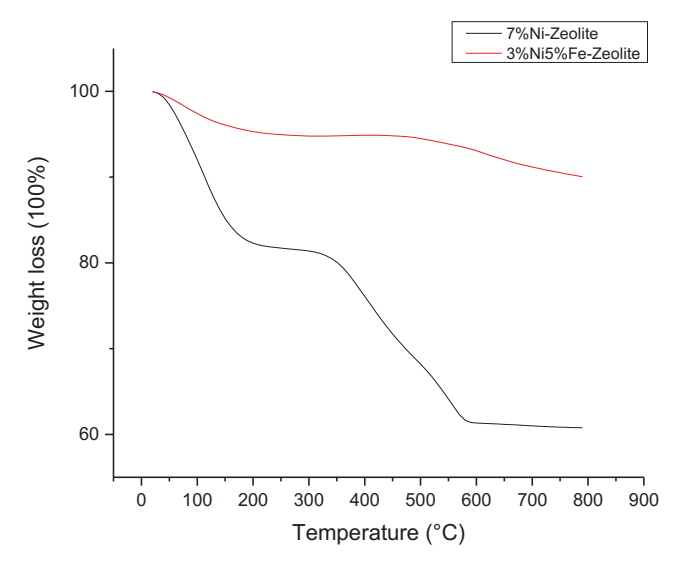


Fig. 4. TGA of spent mono and bimetallic catalysts.

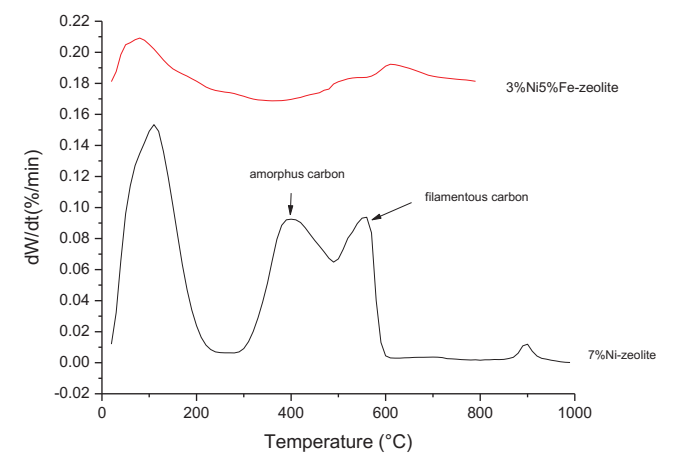


Fig. 5. DSC of spent mono and bimetallic catalysts.

oxidation state is detected around  $600\,^{\circ}$ C. It is observed that the two carbon phases are formed over the monometallic Ni-based catalyst surface; however, addition of iron suppressed the deposition of carbon over the bimetallic Ni-based catalyst.

## 3.2. Steam reforming of toluene activity and stability

In Fig. 6, the reaction reflects the toluene conversion for different catalysts. The catalytic activity of pure zeolite was studied to verify the

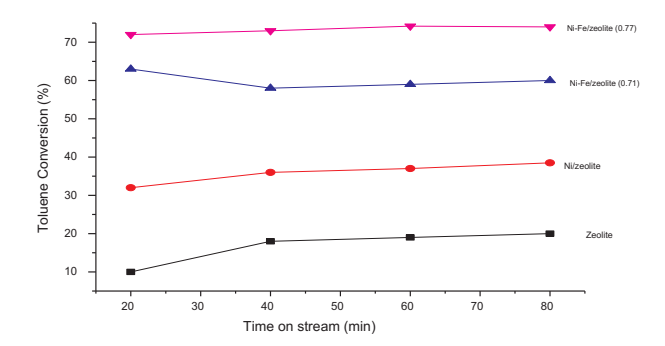


Fig. 6. Toluene conversions versus time-on-stream for several catalyst combinations over zeolite at  $873~\mathrm{K}$ .

catalytic activity with and without active components. The reaction was performed at 873 K with a steam-to-carbon ratio of 3:1. As shown in Fig. 6, Fe promoted the Ni/zeolite catalyst. The catalytic performances obtained at 873 K for the first 80 min are ranked in the order of Ni-Fe/zeolite (0.77) > Ni-Fe/zeolite (0.71) > Ni/zeolite > only zeolite. It was also observed that different catalysts showed slight differences in behavior during the 80 min run time. Despite having lower conversion of about 18%, the conversion over zeolite (pure support) increased slightly from 9% to 18% and then remained almost stable for 80 min. In contrast, Ni-Fe/zeolite (0.71) showed an initial conversion of 63%, reaching a peak conversion of 60% before decreasing slightly. On the other hand, Ni-Fe/zeolite (0.77) had an initial conversion of 72% reaching 74% at 60 min, which subsequently decreased slightly before hovering near 72% conversion.

A quantitative analysis was carried out to determine the composition of products resulted from tar reforming. The retention times of the peaks, the product gases assigned, and their corresponding concentrations were accurately recorded. Part of synthesized mono, bi, and promoted dual-function catalysts including 7% Ni/zeolite, 15% Fe/zeolite, 5% Ni-7% Fe/zeolite, and 5% Ni-7% Fe-9%Mg/zeolite were tested for toluene cracking at 873 K. It should be noted that the cracking reaction with zeolite was carried out for comparison purposes only. The toluene conversion, as well as the product distribution at initial time and after 10 h of operation, were recorded and analyzed. The main gaseous products of catalytic cracking of toluene were  $\rm H_2$ ,  $\rm C_2H_4$ ,  $\rm C_2H_6$ , and  $\rm C_3H_6$ .

Since Ni-Fe/zeolite (0.77) catalyst showed the highest conversion of toluene among other catalysts, it was chosen for further catalytic analysis. Fig. 7 shows the catalytic performance of Ni-Fe/zeolite in steam reforming of tar at 1073 K. The catalytic performance was evaluated for 60 min in the activity test. The formation rate of the gaseous products was almost stable during 15 min. In the case of Ni/zeolite, the amount of the residual tar was large and the H<sub>2</sub>/CO ratio was rather low. These behaviors represent the low steam reforming activity of monometallic catalyst (Ni/zeolite). The addition of Fe to Ni/zeolite promoted the steam reforming reaction monotonously in the range of the molar ratio of Ni to Fe (Ni/Fe)  $\leq$  0.7, and the amount of tar decreased. In contrast, the excess addition of Fe (Ni/Fe > 0.7) significantly decreased the formation rate of gaseous products. The catalytic activity of Ni/zeolite in the steam reforming of tar, which is reflected by unconverted tar amount, is highest at Ni/Fe = 0.77, and the addition of Fe on the steam reforming process has both promoting and suppressing effects. It should be noted that Fe/zeolite exhibited very low activity, under the specified reaction condition, although iron-based catalysts have been investigated in literature and showed effective to the tar reforming. High activity of Ni/zeolite can be caused by synergy between Ni and Fe. The bimetallic catalysts (Ni-Fe) derived from Zeolite supports was effective to methane reforming. In addition, the effect of Fe addition on the coke deposition is more remarkable over Ni/zeolite catalysts with larger amount of Fe addition, although the amount of deposited carbon was large on Ni/zeolite (monometallic catalysts).

T. Ahmed et al. Fuel 211 (2018) 566-571

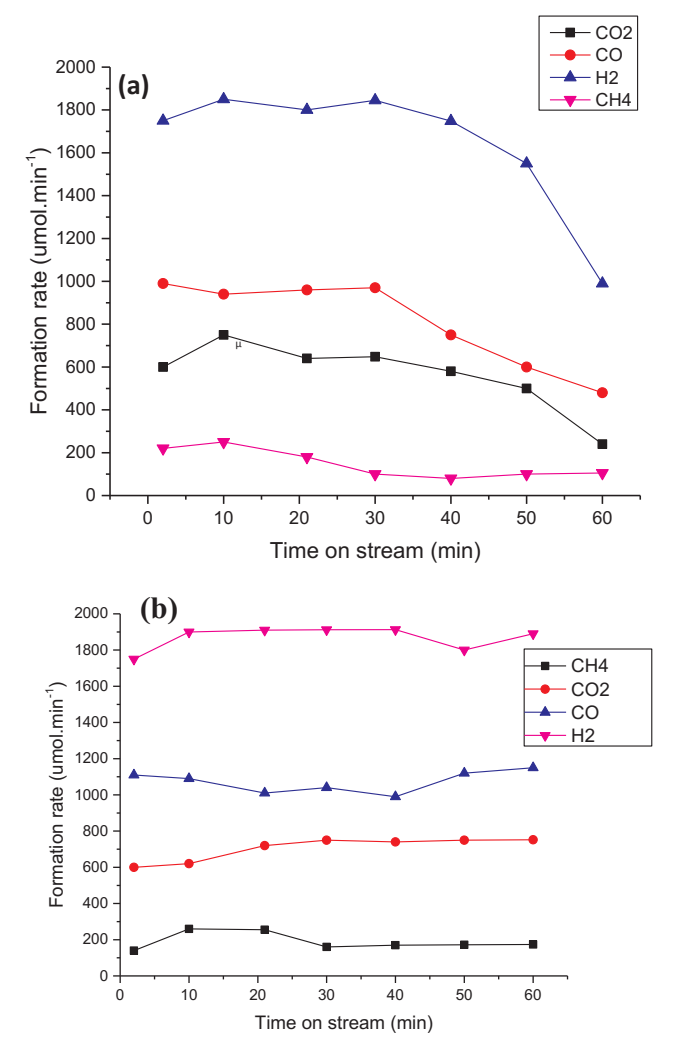


Fig. 7. Reaction time dependence of steam reforming of tar at 1073 K over: (a) Ni (7 wt %) zeolite and (b) Ni-Fe/zeolite (Ni/Fe = 0.77) (Ni 7 wt%).

In Fig. 8(a & b), the SRT has been tested under prolonged time-onstream to investigate the stability of mono and bimetallic catalysts. It is noted that the monometallic catalysts experienced inconsistency in the formation rates of gaseous products. This is due to the formation of the filamentous and amorphous carbons over the active sites. It can be shown that the catalytic activity approached the deactivation stage after 200 min, whereas, the bimetallic catalyst maintained the catalytic efficiency at higher time-on-stream stages (Fig. 9)

# 3.3. Effect of $H_2O/C$ on hydrogen yield

The monometallic and bimetallic catalysts have shown good catalytic cracking properties. However, the hydrogen yields ranged only 55–65% (Fig. 7). The lower hydrogen yield can be attributed to the low number of basic sites through these catalysts. Therefore, a good candidate was magnesium. According to the basic nature between nickel, iron, and magnesium, stronger basic catalytic sites would be synthesized when magnesium was added to these metals. It was observed that the addition of magnesium to the Ni-Fe/zeolite at a molar ratio of H<sub>2</sub>O/C, close to 1:1, yielded the highest reforming of 86%. However, a higher H<sub>2</sub>O/C molar ratio of more than 1:1 resulted in lower hydrogen yield. This phenomenon is due to the oxidant/hydrocarbon content in the feed. At operating condition with high H<sub>2</sub>O/C ratios, the catalyst behaves like oxide-base catalysts, which provide low catalytic reforming activity.

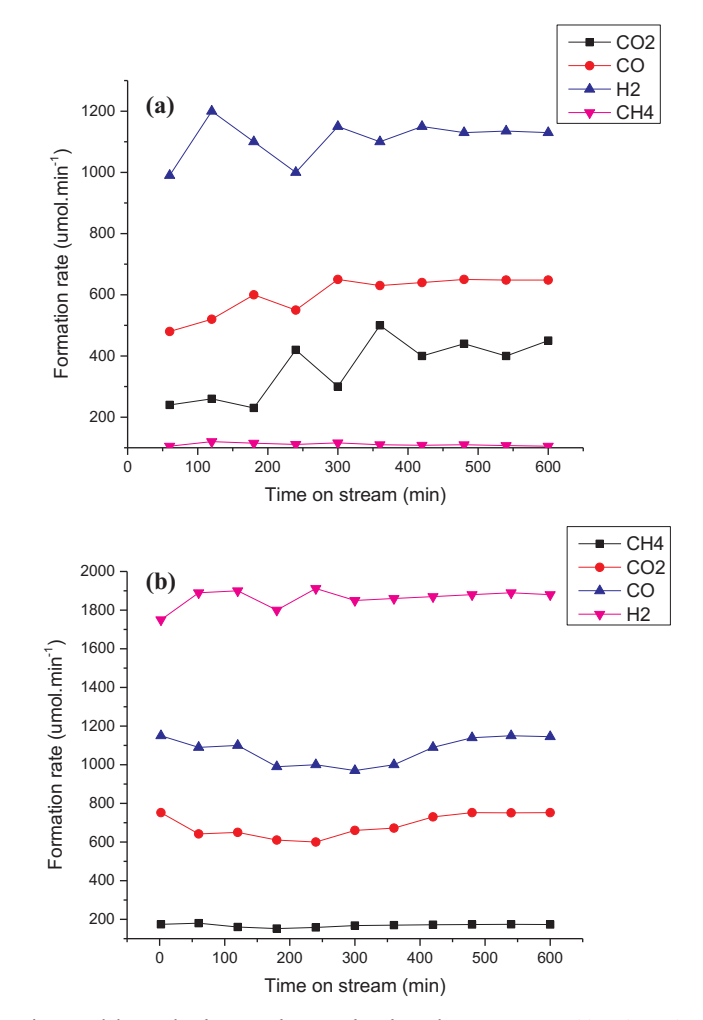


Fig. 8. Stability study of steam reforming of tar for 10 h at 1073 K over: (a) Ni (7 wt%)/zeolite and (b) Ni-Fe/zeolite (Ni/Fe = 0.77) (Ni 7 wt%).

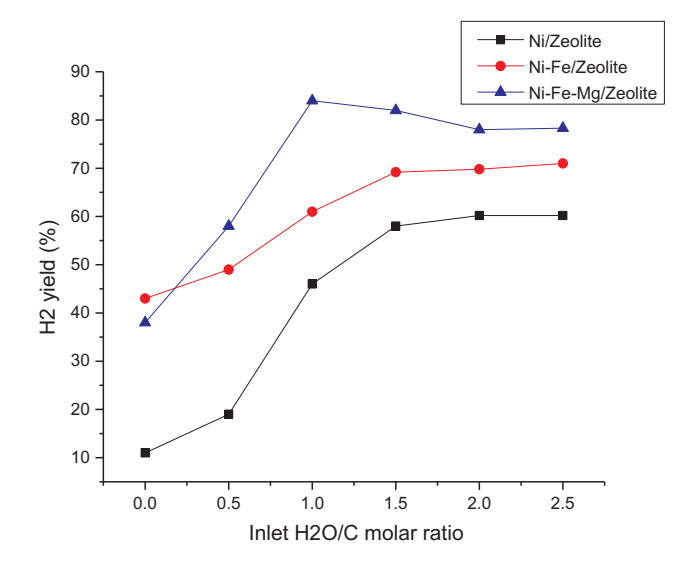


Fig. 9. Effect of inlet  $H_2O/C$  on  $H_2$  yield from the steam reforming of toluene over several catalysts compositions at 1073 K.

# 4. Conclusions

Steam reforming of toluene (SRT) as a biomass tar model compound was investigated over Ni/zeolite, Ni-Fe/zeolite, and Ni-Fe-Mg/zeolite

T. Ahmed et al. Fuel 211 (2018) 566–571

catalysts. The addition of Fe to Ni enhanced SRT performance in terms of suppressing coke deposition and improving stability. It has been shown that iron indeed promoted the reducibility of the Ni species. However, low catalytic activity has been observed in the Ni-Fe/zeolite catalyst. The lower SRT catalytic activity of Ni-Fe/zeolite is due to the depletion in basicity strength of this catalyst composition. The composition of the Ni-rich surface with loaded Mg enhanced SRT in terms of coke suppression and catalytic activity. The high catalytic activity of the N-Fe-Mg/zeolite catalyst can be attributed to the presence of free surface Ni metals compared to the Ni-Fe/zeolite catalyst. Finally, these Ni-Fe/zeolite and Ni-Fe-Mg/zeolite catalysts have great potential for application in the steam reforming of biomass tar.

## Acknowledgement

This project was fully supported by funds provided by an NSF-CREST Project (Award Number: 1242152) and DOE (Award Number: EE0003138). Its contents are solely the responsibility of the authors and do not necessarily represent the official views of the funding agency.

## References

- Ashok J, Kawi S. Steam reforming of toluene as a biomass tar model compound over CeO2 promoted Ni/CaO-Al2O3 catalytic systems. Int J Hydrogen Energy 2013;38(32):13938-49.
- [2] Kaewpanha M, et al. Steam reforming of tar derived from the steam pyrolysis of biomass over metal catalyst supported on zeolite. J Taiwan Inst Chem Eng 2013;44(6):1022–6.
- [3] Xu C, et al. Recent advances in catalysts for hot-gas removal of tar and NH3 from biomass gasification. Fuel 2010;89(8):1784–95.
- [4] Laosiripojana N, et al. Development of Ni–Fe bimetallic based catalysts for biomass tar cracking/reforming: effects of catalyst support and co-fed reactants on tar conversion characteristics. Fuel Process Technol 2014;127:26–32.
- [5] Chen T, et al. CO2 reforming of toluene as model compound of biomass tar on Ni/ Palygorskite. Fuel 2013;107:699–705.
- [6] Koike M, et al. Catalytic performance of manganese-promoted nickel catalysts for

- the steam reforming of tar from biomass pyrolysis to synthesis gas. Fuel 2013;103:122-9.
- [7] Kong M, et al. Experimental study of Ni/MgO catalyst in carbon dioxide reforming of toluene, a model compound of tar from biomass gasification. Int J Hydrogen Energy 2012;37(18):13355–64.
- [8] Li C, Hirabayashi D, Suzuki K. Development of new nickel based catalyst for biomass tar steam reforming producing H2-rich syngas. Fuel Process Technol 2009;90(6):790-6.
- [9] Blanco PH, et al. Characterization and evaluation of Ni/SiO2 catalysts for hydrogen production and tar reduction from catalytic steam pyrolysis-reforming of refuse derived fuel. Appl Catal B 2013;134–135:238–50.
- [10] Guan G, et al. Catalytic steam reforming of biomass tar over iron- or nickel-based catalyst supported on calcined scallop shell. Appl Catal B 2012;115–116:159–68.
- [11] Sun L, et al. Preparation and evaluation of Jatropha curcas based catalyst and functionalized blend components for low sulfur diesel fuel. Fuel 2017;206:27–33.
- [12] Wang L, et al. Catalytic performance and characterization of Ni–Co catalysts for the steam reforming of biomass tar to synthesis gas. Fuel 2013;112:654–61.
- [13] Josuinkas FM, et al. Steam reforming of model gasification tar compounds over nickel catalysts prepared from hydrotalcite precursors. Fuel Process Technol 2014;121:76–82.
- [14] Li D, et al. Metal catalysts for steam reforming of tar derived from the gasification of lignocellulosic biomass. Bioresour Technol 2015;178:53–64.
- [15] Ashok J, Kawi S. Steam reforming of biomass tar model compound at relatively low steam-to-carbon condition over CaO-doped nickel–iron alloy supported over iron–alumina catalysts. Appl Catal A 2015;490:24–35.
- [16] Wang C, et al. Steam reforming of biomass raw fuel gas over NiO-MgO solid solution cordierite monolith catalyst. Energy Convers Manage 2010;51(3):446-51.
- [17] Li D, Nakagawa Y, Tomishige K. Development of Ni-based catalysts for steam reforming of tar derived from biomass pyrolysis. Chin J Catal 2012;33(4–6):583–94.
- [18] Oemar U, et al. Perovskite La x M 1 x Ni 0.8 Fe 0.2 O 3 catalyst for steam reforming of toluene: crucial role of alkaline earth metal at low steam condition. Appl Catal B 2014:148:231-42.
- [19] Oemar U, et al. Promotional effect of Fe on perovskite LaNi x Fe 1 x O 3 catalyst for hydrogen production via steam reforming of toluene. Int J Hydrogen Energy 2013;38(14):5525-34.
- [20] Ashok J, et al. Bi-functional hydrotalcite-derived NiO-CaO-Al 2 O 3 catalysts for steam reforming of biomass and/or tar model compound at low steam-to-carbon conditions. Appl Catal B 2015;172:116-28.
- [21] Wang Z, et al. Oxidative steam reforming of biomass tar model compound via catalytic BaBi 0.05 Co 0.8 Nb 0.15 O 3 8 hollow fiber membrane reactor. J Membr Sci 2016:510:417–25.
- [22] Li Z, et al. Design of highly stable and selective core/yolk-shell nanocatalysts—a review. Appl Catal B 2016;188:324–41.